Z. Phys. B – Condensed Matter 59, 265–270 (1985)

Condensed Zeitschrift für Physik B Matter

Multivalued Anisotropy of Electric Conductivity in Si Near to the ⟨111⟩-Direction

M. Asche [1], V.M. Ivashenko [2], and V.V. Mitin [2]

[1] Zentralinstitut für Elektronenphysik der AdW der DDR, Berlin, German Democratic Republic

[2] Institute of Semiconductors, Academy of Sciences of the Ukrainian SSR, Kiev, USSR

Received January 11, 1985

The current voltage characteristics and the dependence of the transverse electric field on applied voltage is studied experimentally and theoretically for *n*-Si at 27 K for the current close to the ⟨111⟩-direction. A solution in form of a loop is split off from the solution with nearly equal carrier population in all three valleys and corresponds to predominant population of only one valley. The solutions corresponding to predominant population of either one of the three valleys may coexist in the sample in the form of layers parallel to the current. A transverse magnetic induction B may change the size of the layers and by appropriate B it is possible to induce either one of these three layers or any combination of them into the sample.

1. Introduction

When the intervalley scattering time of the electrons in a many valley semiconductor rapidly decreases with increasing carrier heating by an applied electric field, a multivalued electron distribution (MED) among the equivalent valleys can become realized as proposed in [1, 2]. The theoretical prediction of MED was experimentally proved for the case of two equivalent valleys in Si, which are symmetrically orientated with respect to the $(\bar{1}10)$ plane [3–5] for current directions from ⟨110⟩ up to nearly ⟨111⟩. Under the condition of MED two different distributions of electrons between these two valleys are possible: The first valley is predominantly populated and the second one is almost empty, or the second valley is predominantly populated at the expense of the first one. Equal population of these two valleys, however, is unstable when MED can be realized. The two possible redistributions of the electrons coexist and spontaneously two layers arise in the sample with the interlayer wall parallel to the current. According to the different redistributions of electrons in both layers two different transverse fields result. For symmetrical conditions with regard to the side surfaces the interlayer wall is usually located in the middle of the sample and shifts under the influence of a small transverse magnetic induction to one of the side surfaces. The shift of the interlayer wall and current saturation, which arises on account of negative differential conductivity (ndc) as a result of the transverse electric fields [1], were observed experimentally [3–5].

In [6] and [7] special attention was drawn to the current directions in the neighbourhood of ⟨111⟩. In contrast to the two-valley case firstly there are now three pairs of equivalent valleys (furtheron described as three valleys) and consequently three possible redistributions with predominant population of either one of these three valleys. Further the theoretical considerations show that for MED and for the chosen parameters characterising the intervalley scattering one of the stable solutions is given by equal population of these three valleys and the other stable solutions by predominant population of either one of these three valleys represented by parts of loops isolated from the solution with equal population of the valleys. These loops increase, when the intervalley scattering probability of the electrons on impurities decreases.

For certain boundary conditions on the side surfaces, however, the stable solution of equal population of the valleys is not realised, but the transition into the part of the isolated loops which belongs to the strongest repopulation into one of the valleys becomes possible. In [8] the results of an experimental

observation of MED of this type were published. Detailed theoretical as well as experimental investigations of this problem have been performed since then and their results are presented in Sects. 2 and 3.

2. Experimental Results

The measurements were performed in accordance with [4, 8]. The samples of Si highly purified with respect to the residual acceptor concentration were cut from the $(\bar{1}10)$ plane and the current contacts and the side probes were alloyed to the sample as shown in Fig. 1. The samples were immersed in liquid neon.

On account of the small declination of the current direction from ⟨111⟩ (see Fig. 1) one of the valleys (called the third furtheron) is distinguished with respect to both the others. Figure 2 shows the dependence of the transverse voltage drop ΔU_{i-j} devided by the distance of the probes d_{i-j} measured along the y- and z-directions as a function of average longitudinal electric field $\bar{E}=U/l$ with U equal to the applied voltage and l being the sample length. In the absence of a magnetic induction (as shown in [8]) due to the small deviation of the current direction from ⟨111⟩ the predominant population of valley 1 or 2 (see Fig. 1) is possible. Because these valleys are located with their rotation axis under an angle with respect to the axes y and z on account of the conductivity anisotropy both field components E_y and E_z arise in the sample. Therefore there are voltage drops between the probes on the pair of $(\bar{1}10)$ surfaces (ΔU_{5-6}) and between the probes on the other pair of side surfaces (ΔU_{12-11}). As the interlayer wall is shifted towards one of the $(\bar{1}10)$ the opposite E_y-components connected with one and the other of the valley populations do not compensate each other. The region of applied electric fields, for which the transverse fields appear, is strongly pronounced and related to the loop character of the solutions as discussed in the next section. In order to check the proposed nature of the effect experimentally weak magnetic inductions are applied parallel to the z- as well as y-axes of the sample.

A magnetic induction applied in the $(\bar{1}10)$ plane perpendicular to the current direction (i.e. along the y-axis) plays the same role as previously in the two-valley case [2–5]: besides the Hall effect the main effects is the shift of the interlayer wall towards one or the other surface perpendicular to the z-axis. For $B=\pm 0.0186\,T$ shown in Fig. 2 the interlayer wall is already shifted to one or the other surface, respectively, and therefore the curve 2 and 3 for $\Delta U_{5-6}/d_{5-6}$ are only opposite in sign, but else equal for both polarities of **B**. It is to be seen that the region of applied electric fields for the steep rise of

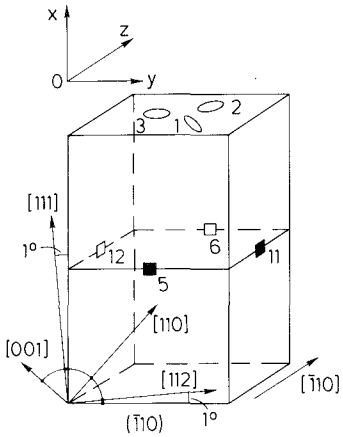

Fig. 1. Orientation of the sample and position of the probes. A projection of the equienergetic surfaces of the valleys on the $z=0$ plane is indicated

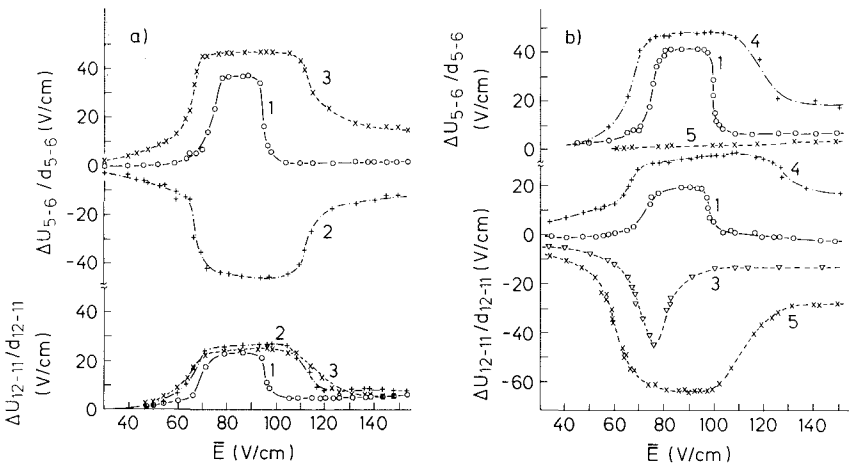

Fig. 2a and b. Transverse voltage drops between indicated probes divided by the distance between these probes as a function of averaged applied electric field $\bar{E}$ for a magnetic induction B along the y-axis (**a**) and along the z-axis (**b**): $B=0$ (1), 0.0186 T (2), −0.0186 (3), 0.037 (4), −0.037 T (5)

the transverse electric field E_z is enlargened with growing magnetic induction in contrast to the two-valley case and reflects the enlargement of the loops with **B**, but this behaviour will not be discussed in detail for this orientation.

With regard to $E_y = \Delta U_{12-11}/d_{12-11}$ the polarity of **B** plays no role, of course, and the magnitude of B changes only the region of applied electric fields for which the transverse fields appear according to the already mentioned effect of **B** on E_z.

The orientation of **B** along the z-axis is more interesting since the situation significantly changes in comparison to the two-valley case. For the polarity of **B**, which turns the electric field towards ⟨110⟩ the situation is similar to that described above, i.e. the region of $\bar{E}$ for which MED is realized, increases with B (curve 4 in Fig. 2b). However, for that polarity, which turns the electric field towards ⟨111⟩ the predominant population of the third valleys becomes realized. This time there appears a layer according to the solution for the predominant population of the third valley besides both the others. It is characterized by another E_y with regard to sign as well as value than in the preceeding case and the lack of E_z, because the rotation axis of the third valley lies in the $x-y$-plane (see projections of the valleys indicated in Fig. 1). This situation is clearly exhibited by the curves 5 in Fig. 2b, which demonstrate a high field component in the y-direction $\Delta U_{12-11}/d_{12-11}$ as the layer with prevailing population of the third valley extends almost through the whole sample, but almost no voltage difference along the ⟨$\bar{1}$10⟩ direction. The magnetic induction necessary to turn the electric field strength from the applied direction to ⟨111⟩ and further depends on the value of the heating field, obviously a weaker B is sufficient for lower values of $\bar{E}$ than for higher ones as to be seen from curves 3 and 5 in Fig. 2b.

In order to demonstrate the value of the magnetic induction which is necessary to switch the multivalued states, the dependence of $\Delta U_{i-j}/d_{i-j}$ as functions of B is shown in Fig. 3 for several values of the averaged applied field strength $\bar{E}$ for the case of B parallel to the z-axis (i.e. along ⟨$\bar{1}$10⟩). While below a critical value for $\bar{E}$, for which the steep rise of transverse fields is realized (Fig. 2b), only an ordinary Hall effect is observed as shown by curve 1 in Fig. 3, the behaviour of $E_y(B)$ and $E_z(B)$ described above is obvious for electric field strengths within a certain region and is characterized by the steep "switching" branch for small inductions, as exhibited by curve 2 in Fig. 3 for $\bar{E} = 85$ V/cm. For applied electric fields above a second critical value, for which MED vanishes, the switching effect cannot be observed anymore, and it remains only an anomalous Hall effect due to the strong redistributions among the valleys but without the layered structure of MED (curve 4 in Fig. 3).

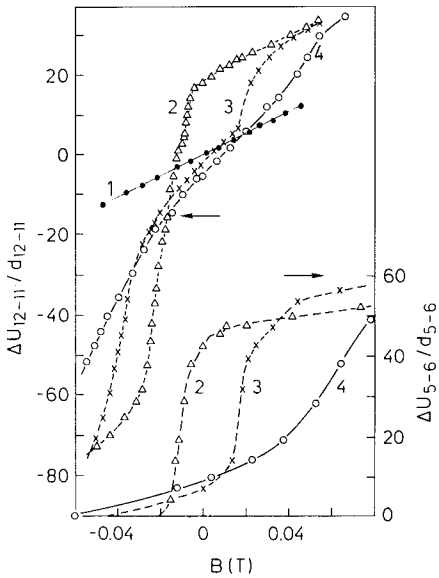

Fig. 3. Transverse voltage drops between indicated probes divided by the distance between these probes as functions of a magnetic induction parallel to the z-axis with average applied electric field $\bar{E}$ as a parameter: $\bar{E} = 43$ V/cm (1), 85 (2), 114 (3), 148 V/cm (4)

On account of the anisotropy of the conductivity the appearance of transverse fields is accompanied by ndc [1, 6], which in long time measurements leads to a region of applied electric fields with current saturation as observed earlier [3–8]. At $\bar{E} = E_l$ the static high field domain due to ndc is nucleated at one contact and extends further into the sample with growing $\bar{E}$. When the static high field domain extends through the whole sample ($\bar{E} = E_c$) the current density begins to rise slowly with further growing $\bar{E}$, as long as the applied electric field strength is still smaller than the upper critical value E_h for MED, i.e. for the disappearance of the transverse electric fields. For $\bar{E} \geqq E_h$ the current steeply rises up to values, which correspond to the absence of MED, as to be estimated by extrapolation of the curve from the region $\bar{E} \leqq E_l$.

For the magnetic induction along the y-axis the saturation current decreases with growing B and a small linear dependence on B arises, i.e. as expected the depence of the current voltage characteristics on B is the same as for the two-valley situation considered earlier [3, 4] and will not be described in detail therefore.

For the magnetic induction parallel to ⟨$\bar{1}$10⟩ for the polarity, which favours the MED between the first and second valley, E_l is shifted to lower values in accordance with the appearance of the transverse

fields (curves 4 in Fig. 2b) and the value of the saturation current diminishes (curve 2 in Fig. 4). However, for that polarity, which leads to MED between the third valley and one of the other valleys, the current density increases for small B and the saturation character vanishes already for B of about 10^{-2} T. This situation is depicted by curve 3 in Fig. 4. When B grows further the current density decreases and again a plateau develops. For $B=0.037$ T (i.e. twice the value of curve 3) the current exhibits as well pronounced saturation region below the value of the saturation current for $B=0$.

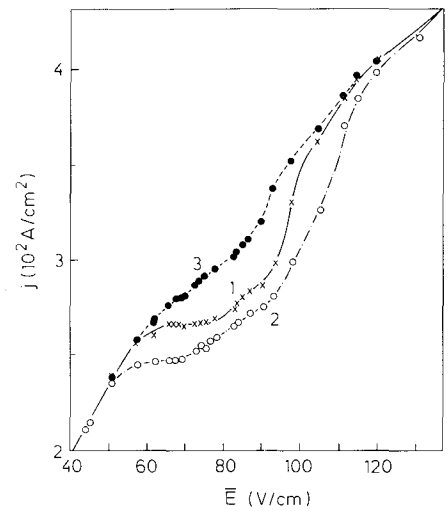

Fig. 4. Current density j versus average applied electric field $\bar{E}$ for $B=0$ (1), and $\mathbf{B}//z$ (2, 3), $B=0.0186$ T (2), $B=-0.0186$ T (3).

3. Numerical Calculations and Discussions of the Results

To calculate the intervalley repopulation of electrons, the transverse electric fields, and the current voltage characteristics, the transport equation was solved by Monte Carlo simulations as in [4, 9] in the presence of an electric field $\mathbf{E}$ and a transverse magnetic induction $\mathbf{B}$. We use the Herring-Vogt transformation, which reduces the ellipsoidal equienergetic surfaces of the valleys α to spheres:

$$p_{1,2}^{(\alpha)}=\left(\frac{m}{m_t}\right)^{1/2}p_{1,2},\qquad p_3^{(\alpha)}=\left(\frac{m}{m_l}\right)^{1/2}p_3 \tag{1}$$

$$V_{1,2}^{(\alpha)}=\left(\frac{m_t}{m}\right)^{1/2}V_{1,2},\qquad V_3^{(\alpha)}=\left(\frac{m_l}{m}\right)^{1/2}V_3,$$

$$m=(m_t^2 m_l)^{1/3}. \tag{2}$$

Here $\mathbf{p}^{(\alpha)}$ and $\mathbf{V}^{(\alpha)}$ are the transformed wave vector and velocity in the reference frame centered at the bottom of the valley with axis 3 along the longitudinal axis, m_l and m_t being the longitudinal and transverse components of the effective mass tensor, of course. Applying this transformation to $\mathbf{E}$ and $\mathbf{B}$, the effective electric field $\mathbf{E}^{(\alpha)}$ and magnetic induction $\mathbf{B}^{(\alpha)}$ in the valley α read:

$$E_{1,2}^{(\alpha)}=\left(\frac{m}{m_t}\right)^{1/2}E_{1,2},\qquad E_3^{(\alpha)}=\left(\frac{m}{m_l}\right)^{1/2}E_3 \tag{3}$$

$$B_{1,2}^{(\alpha)}=\frac{m}{(m_t m_l)^{1/2}}B_{1,2},\qquad B_3^{(\alpha)}=\frac{m}{m_t}B_3. \tag{4}$$

The transformation preserves the orthogonality of the electric field and magnetic induction ($\mathbf{E}^{(\alpha)}\times\mathbf{B}^{(\alpha)}=\mathbf{E}\times\mathbf{B}$), and for isotropic scattering $\mathbf{E}^{(\alpha)}$ and $\mathbf{B}^{(\alpha)}$ characterise the transport properties of the electrons in valley α [4]. The transport equation in each valley was solved and the dependence of the mean velocity $\bar{V}^{(\alpha)}$ and of the intervalley out-scattering time on phonons $\tau^{(\alpha)}$ on $\mathbf{E}^{(\alpha)}$ were obtained. The results

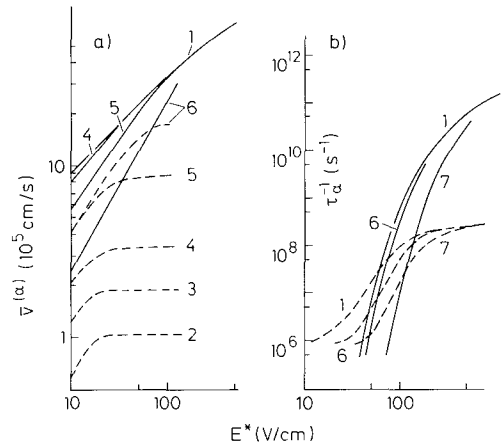

Fig. 5a and b. The components of the effective drift velocity in a valley $\bar{V}_{\parallel}^{(\alpha)}$ (solid curve) (**a**) and $\bar{V}_{\perp}^{(\alpha)}$ (dashed curve) (**a**) and the reciprocal intervalley scattering time on the f_2+f_3-phonons (solid curve) and on the f_1-phonons (dashed curve) (**b**) versus effective electric field strength $E^*=E^{(\alpha)}$ in a valley α. With the effective magnetic induction $B^{(\alpha)}$ as a parameter: $B^{(\alpha)}=0$ (1), 0.0075 T (2), 0.015 (3), 0.03 (4), 0.08 (5), 0.18 (6), 0.38 T (7)

are presented in Fig. 5. The two components of the velocity $\bar{V}_{\parallel}^{(\alpha)}$ along $\mathbf{E}^{(\alpha)}$ and $V_{\perp}^{(\alpha)}$ along $\mathbf{E}^{(\alpha)}\times\mathbf{B}^{(\alpha)}$ are shown separately. The intervalley-out-scattering times $\tau_i^{(\alpha)}$ are presented for interaction with low energy phonons ($\hbar\omega_{f_1}=18$ meV) described as $\tau_1^{(\alpha)}$ and with high energy phonons ($\hbar\omega_{f_2}=47$ meV and $\hbar\omega_{f_3}=59$ meV) described as $\tau_2^{(\alpha)}$, with the electron phonon coupling constants according to [4, 9].

For $B^{(\alpha)}\gtrsim 0.06$ T the values of $\bar{V}_{\parallel}^{(\alpha)}$ and $\tau_i^{(\alpha)-1}$ decrease with increasing magnetic induction. It is to be noticed that with increasing $B^{(\alpha)}$ the effective electric field $E^{(\alpha)}$ increase, too, as they include the applied electric field as well as all the components arising in the sample. For very high values of $E^{(\alpha)}$ the $\tau_i^{(\alpha)-1}(B)$

and $\bar{V}_{\parallel}^{(\alpha)}(B)$ tend to the curves for $B=0$. For $B^{(\alpha)} \lesssim 0.06\,\mathrm{T}$ – the region of interest for the comparison with experimental data – for $\bar{V}_{\parallel}^{(\alpha)}$ and $\tau_i^{(\alpha)-1}$ their values at $B=0$ can be used. On the other hand $\bar{V}_{\perp}^{(\alpha)}$ is proportional to $B^{(\alpha)}$ in this region of magnetic induction and depends linearly on $E^{(\alpha)}$ for $E^{(\alpha)} \lesssim 20\,\mathrm{V/cm}$ with $\bar{V}_{\perp}^{(\alpha)}/E^{(\alpha)}B^{(\alpha)} = 8\times10^5\,\mathrm{cm^2/Vs\,T}$ and is independent from $E^{(\alpha)}$ for $E^{(\alpha)} \gtrsim 25\,\mathrm{V/cm}$ with $\bar{V}_{\perp}^{(\alpha)}/B^{(\alpha)} = 1.2\times10^7\,\mathrm{cm/s\,T}$. For high magnetic inductions the behaviour of $\bar{V}_{\perp}^{(\alpha)}$ is more complicated exhibiting maxima, not shown here, as for the experimentally envolved values of $B^{(\alpha)}$ the linear approximation is valid.

For the current voltage characteristics the mean drift velocity V_D was calculated as a function of applied electric field E_x. The results are shown in Fig. 6a. Curve D represents the drift velocity for equal population of the valleys. The predominant population of one of the three valleys leads for the current directed exactly along ⟨111⟩ to the threefold degenerated solution C in the form of an isolated loop. Only the lower part of the loop, which corresponds to the strongest repopulation of electrons and the largest transverse fields consequently (see Fig. 6e) is stable. Here and furtheron the stable solutions are depicted by solid lines and the unstable ones by broken lines. The stability of the solutions was verified as in [1, 2]. Solutions in the form of isolated loops are obtained, if the intervalley scattering probability τ_0^{-1} of the electrons on ionised impurities is small in comparison to that on phonons. Our calculations show that isolated loops exist if $\tau_0^{-1} \lesssim 5\times10^7\,\mathrm{s^{-1}}$. As already stated in [6] a good agreement between enumerated and experimentally determined curves is achieved for $10^7 \lesssim \tau_0^{-1} \lesssim 10^8\,\mathrm{s^{-1}}$. Therefore furtheron theoretical results are demonstrated for $\tau_0^{-1} = 10^7\,\mathrm{s^{-1}}$. – For a small deviation of the current from ⟨111⟩ by $\varphi = 1°$ towards ⟨110⟩ the threefold degenerated loop C is splitted into a twofold degenerated loop B, which corresponds to a predominant population of the valleys 1 or 2, and a loop A for a repopulation of the electrons into the valley 3. Only for a small region of φ solution A can be realized, with increasing φ the loop A is quickly narrowed and vanishes while the loop B increases with growing φ until it merges into curve D and a behaviour with negative differential conductivity (ndc) as for the ⟨110⟩ direction results [7].

Fig. 6b, c depicts the influence of a magnetic induction along ⟨$\bar{1}$10⟩ for that polarity of the magnetic induction which turns the resulting electric field towards ⟨001⟩. The solutions of the types B and A are presented separately in Fig. 6b and 6c for sake of clearity. The twofold degenerated loops B corresponding to the redistribution into valley 1 or 2 narrow with increasing magnetic induction and vanish for $B \approx 0.018\,\mathrm{T}$, while the loop A corresponding to the redistribution into valley 3 blows up and merges into curve D. For magnetic inductions above 0.02 T only a monovalued behaviour remains in accordance with the effect that the electric field was already turned away from ⟨111⟩ towards ⟨001⟩.

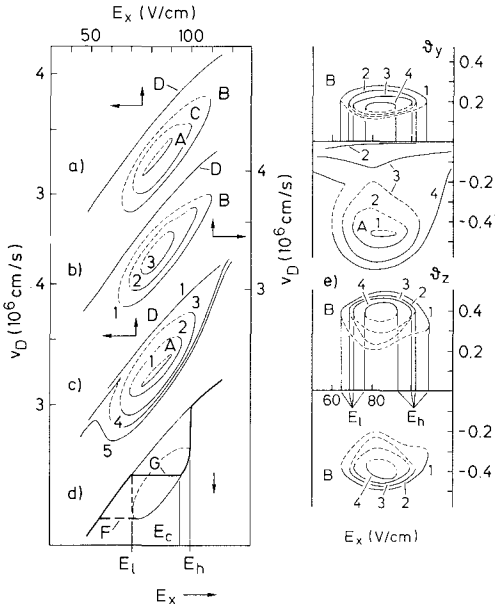

Fig. 6a–e. Drift velocity V_D averaged over the valleys as a function of applied electric field strength E_x: **a**, **b** and **c** for a homogeneous distribution of the electric field strength, **d** for an inhomogeneous distribution, and dependence of the ratio of the transverse electric field strength to the applied one $\vartheta_y = E_y/E_x$, $\vartheta_z = E_z/E_x$ versus E_x. The magnetic induction is directed along the z axis: $B=0$ (1), 0.005 T (2), 0.01 (3), 0.015 (4), 0.02 T (5)

For the other polarity of the magnetic induction the A loop vanishes quickly, while the B loops are widened until they merge with curve D. With further growing magnetic induction there remains MED between the valleys 1 and 2, but not with loop character, and we do not present these results here. The transverse electric fields corresponding to Fig. 6b–c are depicted in Fig. 6e. If the field distribution is a priori assumed to be homogeneous with respect to y and the influence of the valley 3 proposed to be neglegible then with respect to the discussion of E_z the two-valley model of [2, 7, §33] is realized. For small intervalley scattering velocities at least on one of the ($\bar{1}$10) surface a solution $E_z = 0$ cannot be realized in the region $E_l \leqq E \leqq E_h$, but only the upper branch of loops B corresponding to a population valley 2 with $\vartheta_z = E_z/E_x > 0$ or the lower branch of loops B for the population of valley 1 with $\vartheta_z < 0$ are stable solutions. The sample is split up into two layers parallel to ($\bar{1}$10) according to both the stable solutions with a steep interlayer wall between them or when

the wall is shifted towards one of the $(\bar{1}10)$ surfaces a monolayered structure with predominant population of one of the valleys and consequently a voltage drop across the sample corresponding to either $\vartheta_z > 0$ or < 0 become realized.

The application of a magnetic induction along $\langle\bar{1}10\rangle$, which favours the redistribution of carriers into valley 3, leads to a simultaneous increase of the A loop and a narrowing of the B-loops for the transverse fields. Therefore for not too high magnetic inductions there results a stratification of the sample into two layers, one with electrons according to the B-solution, the other with a carrier redistribution into valley 3 according to the A-solution. The region of electric fields, for which B-loops can be realized, diminishes with increasing magnetic induction and vanishes, and there remains only the transverse field component E_y corresponding to the anisotropy of the conductivity of valley 3.

The presence of the loops in $V_d(E)$ and the transitions from and to the solution with nearly equal population of the valleys at the field strengths E_l and E_h, respectively (Fig. 6d) are mirrored in the current voltage characteristics of Fig. 4. Theoretically two different saturation currents can be realized as shown by lines F and G in Fig. 6d [4]. Such saturation currents may be depicted on each loop in Fig. 6a–c, of course. In the experiment type G is realized, because the current saturation begins just only a little below that value of the electric field E_c for which the switching behaviour for the transverse voltage drop by a magnetic induction is already observed between the probes near to that electrode, at which the static high field domain is built up.

The calculated influence of the magnetic induction represented in Fig. 6 describes the experimental effects in a satisfying way. The current voltage characteristics in the saturation region as well as the behaviour of the transverse field are mirrored correctly by the theoretically obtained loops.

References

1. Gribnikov, Z.S., Kochelap, V.A., Mitin, V.V.: Zh. Eksp. Teor. Fiz. **59**, 1828 (1970) (Sov. Phys. JETP **32**, 991 (1971))
2. Gribnikov, Z.S., Mitin, V.V.: Zh. Eksp. Teor. Fiz. Pis'ma Red. **14**, 272 (1971) (JETP Lett. **14**, 182 (1971)); Fiz. Tekh Poluprovodn. **9**, 276 (1975) (Sov. Phys. Semicond. **9**, 180 (1975)
3. Asche, M., Kostial, H., Sarbei, O.G.: J. Phys. C **13**, L645 (1980)
4. Asche, M., Gribnikov, Z.S., Ivastchenko, V.M., Kostial, H., Mitin, V.V., Sarbei, O.G.: Zh. Eksp. Teor. Fiz. **81**, 1347 (1981) (Sov. Phys. JETP **54**, 715 (1982))
5. Asche, M., Ivastchenko, V.M., Kostial, H., Mitin, V.V.: Fiz. Tekh. Poluprovodn. **18**, 1660 (1984)
6. Asche, M., Gribnikov, Z.S., Ivastchenko, V.M., Kostial, H., Mitin, V.V.: Phys. Status Solidi (b), **114**, 429 (1982)
7. Asche, M., Gribnikov, Z.S., Mithin, V.V., Sarbei, O.G.: Goryachie elektrony v mnogodolinukh poluprovodnikakh. pp. 136–137. Kiev: Naukova dumka 1982
8. Asche, M., Kostial, H.: Phys. Status Solidi (b) **120**, K83 (1983)
9. Jacoboni, C., Regiani, L.: Rev. Mod. Phys. **55**, 645 (1983)
10. Herring, C., Vogt, E.: Phys. Rev. **101**, 944 (1956)

M. Asche
Zentralinstitut für Elektronenphysik
Akademie der Wissenschaften der DDR
DDR-1086 Berlin
German Democratic Republic

V.M. Ivashenko
V.V. Mitin
Institute of Semiconductors
Academy of Sciences of the Ukrainian SSR
SU-252028 Kiev
USSR